product in one or more unimolecular dissociation reactions, of which by far the most common pathway apparently involves the formation of excited benzene ions whose dissociation yields ~68% $\mathbf{c}^{\bullet+}$ and ~32% $\mathbf{a}^{\bullet+}$. The surprisingly high correspondence between the $^{+}NR^{+}$ and $^{+}NR^{-}$ values for the relative quantities of all four isomers produced from 13 precursors indicates a high accuracy for such ^{+}NR isomeric analyses.

Acknowledgment. The authors thank C. Wesdemiotis for advice and experimental results,[20] D. E. Drinkwater, M. Marchetti, R. F. Porter, and F. Turecek for helpful discussions, S. R. Kass for a preprint of ref 18, the National Science Foundation (Grants CHE-8712039 and CHE-9014883) for generous financial support, and the National Institutes of Health (GM16609) for instrumentation.

Decay and Fate of the Hydroxyl Radical Adduct of α-Phenyl-*N*-*tert*-butylnitrone in Aqueous Media†

Yashige Kotake* and Edward G. Janzen‡

Contribution from The National Biomedical Center for Spin Trapping and Free Radicals, Molecular Toxicology Research Program, Oklahoma Medical Research Foundation, 825 Northeast 13th St., Oklahoma City, Oklahoma 73104. *Received June 20, 1991*

Abstract: The lifetime of α-(hydroxylbenzyl)-*tert*-butylaminoxyl, the hydroxyl radical adduct of α-phenyl-*N*-*tert*-butylnitrone (PBN) produced by spin trapping, is measured with an EPR spectrometer at various pH values in phosphate buffer. The decay of the EPR signal of the hydroxyl adduct of PBN is first order with respect to the concentration of the aminoxyl and the decay rate constant is strongly dependent on the pH of the solution. The rate constant increases as a function of increasing pH, indicating that the decay mechanism involves the dissociation of an acidic proton. Clear evidence is obtained that the hydroxyl adduct of PBN spontaneously transforms to *tert*-butylhydroaminoxyl.

As a first line of attack hydroxyl radicals add to the unsaturated functions of available substrates. The rates of addition are extremely fast and approach those of diffusion-controlled reactions. Rate constants for addition to targets have been measured, and little variation is found as a function of structure of the unsaturated site.[1] Nitrone spin traps[2] offer no particular exception to this generalization since the rate constants estimated for addition of hydroxyl radicals fall within the range of values frequently encountered for organic molecules, namely 10^{7}–10^{9} mol L^{-1} s^{-1}.[3-6] Thus in evaluating the analytical usefulness of a spin trap for the detection of hydroxyl radicals, the actual rate constant of the spin trapping reaction is not of great importance since it can be assumed to be fast. Of more relevance is the persistance of the spin adduct and the uniqueness of the EPR spectrum.

One of the most often used nitrone spin traps, α-phenyl-*N*-*tert*-butylnitrone (PBN), produces relatively stable spin adducts of a variety of free radicals. The hydroxyl radical produced in various reactions is readily trapped by PBN:[7-9]

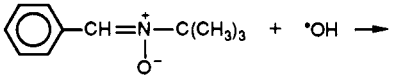

α-phenyl-*N*-*tert*-butylnitrone (PBN)

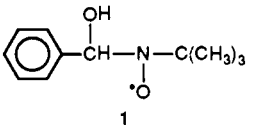

1

α-(hydroxylbenzyl)-*tert*-butylaminoxyl

However, the persistence of the hydroxyl adduct (**1**) may depend on the property of the solubilizing media. In spite of the large number of publications describing experiments utilizing PBN as a spin trap, detailed studies on factors influencing the stability of the hydroxyl adduct have not been published. The fate of the adduct is also unknown. This study is concerned with the decay rates of the hydroxyl spin adduct of PBN produced by the photolysis of hydrogen peroxide in aqueous media as a function of pH and the structure of the primary degradation product obtained in the decay reaction.

Experimental Section

PBN used in this study was synthesized in these laboratories and purified by sublimation before use.[10] Hydrogen peroxide was obtained from Sigma Chemical Co. as a 30% aqueous solution. Distilled water treated with the Millipore MilliQ system was used. D_2O was purchased from KOR Isotopes. The pH of the solution was adjusted by using HCl or KOH in potassium phosphate buffer (0.05–0.1 mol L^{-1}). The solution pH was adjusted after mixing the reagents because hydrogen peroxide usually lowers the pH considerably. Iron-depleted potassium phosphate buffer was prepared by passing 0.05 M buffer through a Chelex 100 column.

A typical experiment involves introducing a solution containing 1% hydrogen peroxide and 4×10^{-3} mol L^{-1} PBN into a flat quartz EPR sample cell. The sample solution was loaded with an injector (Fisher

† Publication No. 1 from the National Biomedical Center for Spin Trapping and Free Radicals.

‡ Departments of Clinical Studies and Biomedical Sciences, Ontario Veterinary College, University of Guelph, Guelph, Ontario, Canada N1G2W1.

(1) For example see: (a) Buxton, G. V.; Greenstock, C. L.; Helman, W. P.; Ross, A. B. *J. Phys. Chem. Ref. Data* **1988**, *17*, 513. (b) Packer, L.; Glazer, A. N., Eds. Oxygen Radicals in Biological Systems. Part B. Oxygen Radicals and Antioxidants. *Methods in Enzymology*; Academic Press: New York, 1990; Vol. 186.

(2) For recent review of spin trapping see: Janzen, E. G.; Haire, D. L. Two Decades of Spin Trapping. In *Advances in Free Radical Chemistry*; Tanner, D., Ed.; JAI Press: Greenwich, CT, 1990; Vol. 1, pp 253.

(3) Finkelstein, E.; Rosen, G. M.; Rauckman, E. J. *J. Am. Chem. Soc.* **1980**, *102*, 4994.

(4) Marriott, P. R.; Perkins, M. J.; Griller, D. *Can. J. Chem.* **1980**, *58*, 803.

(5) Castelhano, A. L.; Perkins, M. J.; Griller, D. *Can. J. Chem.* **1983**, *61*, 298.

(6) Sridhar, R.; Beaumont, P. C.; Powers, E. L. *J. Radioanal. Nucl. Chem.* **1986**, *101*, 227.

(7) Janzen, E. G.; Kasai, T.; Kuwata, K. *Bull. Chem. Soc. Jpn.* **1973**, *46*, 2061.

(8) Harbour, J. R.; Chow, V.; Bolton, J. R. *Can. J. Chem.* **1974**, *52*, 3549.

(9) Janzen, E. G.; Nutter, D. E.; Davis, E. R.; Blackburn, B. J.; Poyer, J. L.; McCay, P. B. *Can. J. Chem.* **1978**, *56*, 2237.

(10) PBN decomposes slowly and forms benzaldehyde in water. When unpurified PBN was used the reproducibility of the rate constants was poor.

0002-7863/91/1513-9503$02.50/0

Figure 1. Resolved hyperfine splitting of the hydroxyl hydrogen in the EPR spectrum of the OH adduct of PBN-d_{14} produced by UV illumination of a phosphate buffer solution of hydrogen peroxide and PBN-d_{14}. Spectrometer settings for EPR measurement are microwave power = 2 mw and field modulation width = 0.1 G.

aqueous Minipet) from the bottom part of the cell. Repeat experiments could be initiated using fresh solution in each case. The hydroxyl adduct was not detected when the solution was placed in the EPR sample cavity. Focused UV light from a 75-W mercury high-pressure arc (ORIEL) was used for illumination without a filter. Approximately 0.5-s exposure time was selected by opening a mechanical shutter. The rise and decay of the EPR signal was monitored at 293 (±1) K by fixing the field at the peak position of the first derivative EPR spectrum. The horizontal axis of the recording was used as a time axis by setting the sweep width to zero. First-order decay rate constants were calculated from the slope of the linear part in the logarithmic plot of the decay. A Bruker ER300 EPR spectrometer equipped with 100-kHz field modulation was used.

Results and Discussion

Assignment of the Hydroxyl Adduct of PBN. Harbour et al.[8] first assigned the EPR spectrum of the hydroxyl adduct of PBN in an aqueous solution from the photolysis of hydrogen peroxide. In order to make sure the aminoxyl radical produced is indeed the hydroxyl adduct, the EPR spectrum was observed after the photolysis of 1% H_2O_2 in the presence of PBN-d_{14}, where PBN is completely deuterated except for the nitronyl hydrogen. The resultant EPR spectrum shown in Figure 1 has an additional small hyperfine splitting (hfs) on all six lines normally observed for PBN spin adducts. This hfs is assigned to the proton on the hydroxyl group.[11] The hfs from the hydroxyl group disappears in 96% D_2O solution even when H_2O_2 is used as a source of the hydroxyl radical. The hydroxyl hydrogen hfs was observed for a wide pH range (pH 5.0–8.8). The hfs's of the hydroxyl adduct are a^N = 15.46 G, $a^H_{\beta H}$ = 2.70 G, a^H_{OH} = 0.21 G for all pH ranges studied.

Dependence of the Decay Rate of the Hydroxyl Adduct on the Concentrations of PBN and Hydrogen Peroxide. The first-order decay rate of the hydroxyl adduct was examined as a function of PBN concentration in the range of 1×10^{-3} to 5×10^{-2} mol L^{-1} in 1% H_2O_2 phosphate buffer solution (pH 7.4). Although the yield of the EPR signal from the hydroxyl adduct increased at higher PBN concentrations, the first-order decay rate constant did not depend on the concentration of PBN. When the concentration of H_2O_2 was increased to higher than 10%, the EPR signal from the hydroperoxyl adduct ($HO_2^{\bullet}$) is superimposed on the spectrum of the hydroxyl adduct.[8,9] Since it is difficult to observe isolated lines of the hydroxyl adduct and the hydroxyl and hydroperoxyl adducts show different decay rates, the decay curve is influenced by the superposition. However, when the H_2O_2 concentration is less than 3%, the time profile of the decay of the hydroxyl adduct does not depend on the concentration of H_2O_2. The presence of Fenton reaction due to the ferrous ion impurity in the phosphate buffer is negligible because no hydroxyl adduct was detected without irradiation. Also no change in decay rate constants was observed when the iron-depleted buffer was used.

Decay Rate of the Hydroxyl Adduct. The decay of the hydroxyl adduct in phosphate buffer solution appears to have no dependence on the concentration of PBN in the concentration range where practical spin trapping experiments are performed. Thus the dependence of the decay rate on pH of the solution was studied

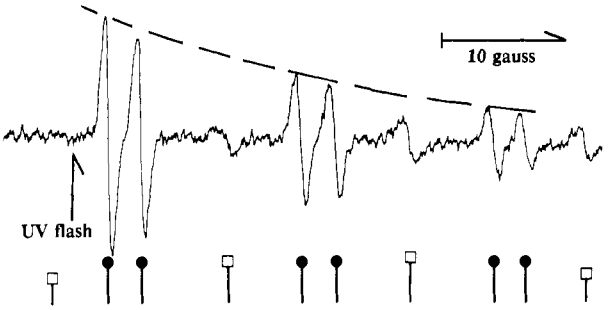

Figure 2. Time course of the rise and decay of aminoxyl radical species after UV illumination of phosphate buffer solution (pH 7.4) of hydrogen peroxide and PBN. UV light was on briefly at the marked position during the magnetic field swept. Total scan time is 42 s. The points indicated with □ are assigned to the *tert*-butylhydroaminoxyl radical; the points indicated with ● denote the hydroxyl adduct of PBN.

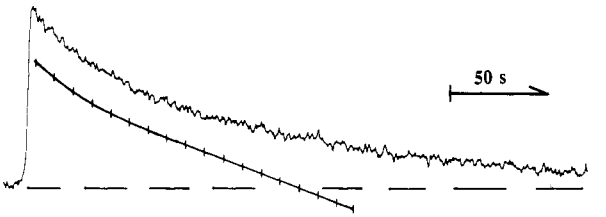

Figure 3. Decay curve of the OH adduct of PBN in phosphate buffer. The plotted curve is logarithmic and consistent with first-order kinetics after about 30 s.

in solutions of 5×10^{-3} mol L^{-1} PBN and 1% (0.29 mol L^{-1}) H_2O_2. When the magnetic field sweep for the EPR measurement was started right after a brief UV illumination, the EPR spectrum shown in Figure 2 was obtained. The decay of the hydroxyl adduct during the field sweep is clearly evident and the spectrum appears to have a weaker doublet at higher field. At the same time a new radical species is identifiable in the spectrum. This radical is assigned to *tert*-butylhydroaminoxyl (**2**) having $a^N = a^H$ = 14.8 G.[12] The time profile of the decay of both aminoxyls **1** and **2**

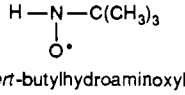

tert-butylhydroaminoxyl

was followed in solutions of various pH. The following characteristic features in the rise and decay of the hydroxyl adduct were observed:

(a) Photolytic Decomposition of the Hydroxyl Adduct. A rapid rise of the EPR intensity of the adduct was observed after UV illumination; however, the intensity level quickly reached a plateau. Prolonged illumination did not produce additional intensity but instead promoted the decay of the spectrum to rates that were much faster than the spontaneous dark decay. It is concluded that the adduct is decomposed by UV illumination.

(b) Order of Decay Kinetics of the Hydroxyl Adduct. Figure 3 shows the decay curve of the EPR intensity of the hydroxyl adduct taken from the third peak at low field in a solution of pH 6.5. The initial part of the trace reveals a different type of decay from that of the remainder. The late part of the decay curve shows good linearity on a logarithmic plot of intensity versus time; however, the initial portion is not linear. This fact has been noted previously in the decay of the hydroxyl adduct of PBN produced by photolysis in acidic solutions.[4] It was reported that the decay of the hydroxyl adduct follows second-order kinetics when the adduct concentration is higher than 2×10^{-4} mol L^{-1}. This second-order decay is believed to be due to disproportionation of two adduct molecules. The present study confirms that when the adduct is produced in high concentrations the number of adduct molecules is decreased according to second-order kinetics consistent

(11) The hfs of the hydroxyl hydrogen has been previously observed in the hydroxyl adduct of PBN-d_{14} produced in an aqueous solution of sodium persulfate. Haire, D. L. Isotope substitution in spin trapping: ^2H and ^{13}C labelling of nitrones and radical addends. Ph.D. Thesis, University of Guelph, 1988.

(12) Kalyanaraman, B.; Perez-Reyes, E.; Mason, R. P. *Tetrahedron Lett.* **1979**, 4809.

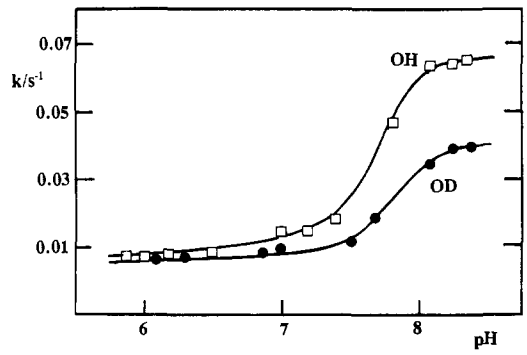

Figure 4. Plot of decay rate constants of the OH adduct of PBN as a function of pH of the solution: (□) OH adduct, (●) OD adduct.

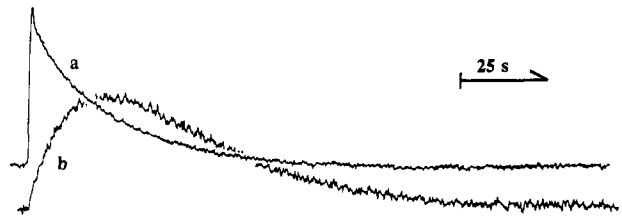

Figure 5. Time profile of formation and decay of *tert*-butylhydroaminoxyl in phosphate buffer (pH 8.2) as compared to that of the OH adduct: (a) OH adduct, (b) *tert*-butylhydroaminoxyl. The sensitivity of the spectrometer was doubled from curve a to curve b.

with disproportionation. The remaining isolated spin adducts decompose by way of first-order kinetics.

(c) pH Dependence of the Decay Rate of the Hydroxyl Adduct. The first-order decay rates of the hydroxyl adduct were measured in solutions of various pH using the same concentrations of PBN (5×10^3 mol L^{-1}) and H_2O_2 (0.29 mol L^{-1}) with the illumination period kept constant. The decay of the EPR signal was observed with the EPR spectrometer settings higher than those for optimum resolution in order to maximize the signal intensity. The initial concentration of the hydroxyl adduct produced by photolysis was kept lower than 1×10^{-5} mol L^{-1} so as to avoid second-order decay. As shown in Figure 4, the decay rate becomes faster as the solution pH is increased. The decay rate constants level off at pH values lower than 6.0 and higher than 8.0. The half-lives at these pH's are 90 and 11 s, respectively. At pH values higher than 9 a new decay path appears and the half-life becomes <1 s. A plot of the half-lives as a function of pH shows features similar to that of a titration curve (Figure 4).

(d) Isotope Effect on the Decay Rate of the Hydroxyl Adduct. The EPR spectrum from the photolysis of H_2O_2 in 96% D_2O solution of PBN-d_{14} shows no hfs from the hydroxyl hydrogen. Hydrogens in H_2O_2 are dissociable and are exchanged rapidly with deuterium. Thus photolysis allows the detection of the EPR spectrum of the deuterioxyl adduct that does not show γ-hydrogen hfs. The degradation product is *tert*-butyldeuterioaminoxyl which has $a^N = 14.8$ G and $a^D_{ND} = 2.30$ G. The decay rate constants of the deuterioxyl adduct of PBN are also plotted in Figure 4. An isotope effect is not significant in the lower pH range. However, the rate constant decreases by about one-third in D_2O when the pH is higher than 8.

(e) Degradation Product of the Hydroxyl Adduct. Formation of aminoxyl **2** was observed in all solutions from the decay of hydroxyl adduct. However, the EPR intensity of **2** is lower in acidic solutions. The rise and decay of the EPR signal from aminoxyl **2** was followed by the same method as for the hydroxyl adduct. Figure 5 shows the time profile of the formation and decay of **2** in a solution of pH 8.2 in comparison to the decay of the hydroxyl adduct. It is clear that the rise of the EPR signal of aminoxyl **2** happens after the UV light is turned off. Aminoxyl **2** appears to be a major degradation product of the hydroxyl adduct based on the fact that the time of maximum decay rate of the OH adduct approximately coincides to that of maximum rate of formation of *tert*-butylhydroaminoxyl. The time course of the concentration of the second product is expressed by[13]

$$[2] = ak_1[\exp(-k_1t) - \exp(-k_2t)]/(k_2 - k_1) \qquad (1)$$

where a is the initial concentration of the hydroxyl adduct, and k_1 and k_2 are the decay rate constants of the hydroxyl adduct (**1**) and *tert*-butylhydroaminoxyl (**2**), respectively. Curve fitting using eq 1 results in $k_2 = 2.3 \times 10^{-2}$ s^{-1} at pH 7.4 and $k_2 = 7.0 \times 10^{-2}$ s^{-1} at pH 8.2.

(f) Decay Mechanism. The fact that the rate constant levels off at both lower and higher pH's indicates that the rate-determining step of the decay mechanism is different at extreme pH values. Thus the decay rate constant k_1 for the hydroxyl adduct at medium pH range can be expressed as[13]

$$k_1 = \frac{K_1[H^+] + k_hK_a}{K_a + [H^+]}$$

where k_h and k_l are the plateau decay rate constants at high and low pH values, respectively, and K_a denotes the ionization constant for the hydroxyl hydrogen of the adduct. The curve shown in Figure 4 can be reproduced by using $k_h = 6.3 \times 10^{-2}$ s^{-1}, $k_l = 7.7 \times 10^{-3}$ s^{-1}, and $K_a = 3 \times 10^{-8}$ mol L^{-1} for the OH adduct and $k_h = 3.9 \times 10^{-2}$ s^{-1}, $k_l = 7.5 \times 10^{-3}$ s^{-1}, and $K_a = 3 \times 10^{-8}$ mol L^{-1} for the OD adduct.

On the basis of the pH dependence of the decay rate, the isotope effect, and the identification of the degradation product the following mechanism can be suggested:

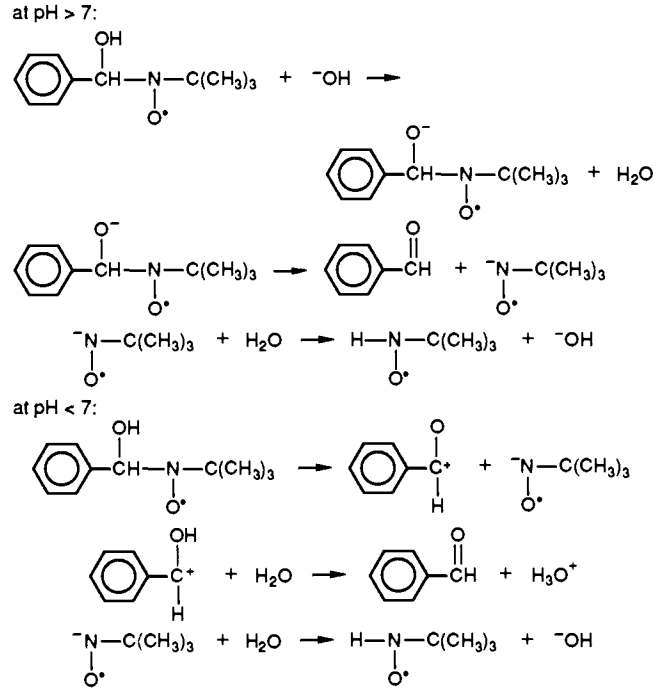

Proton dissociation is not thought to occur in a rapid pre-equilibrium step because the EPR spectrum shows the presence of the hydroxyl proton in the adduct for the whole pH range studied. Thus the rate of association and dissociation in the equilibrium is slower than the EPR time scale (10^6 s^{-1}). In the mechanism proposed the adduct is decomposed into benzaldehyde and the 2-methyl-2-nitrosopropane anion radical. This anion radical is readily protonated to *tert*-butylhydroaminoxyl. The switching of the mechanism with a change in pH of the media is supported by the deuterium isotope effect. At pH greater than 7 the presence of an isotope effect, upon replacing the hydroxyl hydrogen with deuterium to the deuteroxyl group, indicates that the dissociation of the hydroxyl group is rate determining at this pH. On the other hand, the fact that little isotope effect was observed at lower pH suggests the initial step is spontaneous ionic cleavage of the C–N

(13) For example see: Fersht, A. *Enzyme Structure and Mechanism*; W. H. Freeman and Co.: San Francisco, CA, 1977.

bond. Both mechanisms generate *tert*-butylhydroaminoxyl radical.

Acknowledgment. The National Biomedical Center for Spin Trapping and Free Radicals is supported by the Biomedical Research Technology Program of the National Center for Research Resources in National Institutes of Health Grant No. RR05517-01A1. Grateful acknowledgement is hereby made.

Registry No. 1, 55482-05-8; **2**, 22665-15-2; **2-*N*-*d***, 136587-04-7; D_2, 7782-39-0.

Applications of Real-Time FTIR Spectroscopy to the Elucidation of Complex Electroorganic Pathways: Electrooxidation of Ethylene Glycol on Gold, Platinum, and Nickel in Alkaline Solution

Si-Chung Chang,† Yeunghaw Ho, and Michael J. Weaver*

Contribution from the Department of Chemistry, Purdue University, West Lafayette, Indiana 47907. *Received June 19, 1991*

Abstract: The electrooxidation pathways of ethylene glycol in alkaline aqueous solution on gold, platinum, and nickel electrodes are explored by means of real-time FTIR spectroscopy in conjunction with cyclic voltammetry. The former enables a quantitative assay of specific intermediates and products formed during the reaction evolution. The electrooxidation on gold features the successive formation of partially oxidized C_2 solution species en route to oxalate and carbonate production. The latter species is produced predominantly via the formation of the dialdehyde, glyoxal, based on comparisons with electrooxidative spectral sequences for candidate intermediate species. In contrast, ethylene glycol electrooxidation on platinum exhibits markedly different kinetics and product distributions to those for the partially oxidized C_2 species, inferring that at least carbonate production from ethylene glycol occurs largely through sequences of chemisorbed, rather than solution-phase, intermediates. Electrooxidation of ethylene glycol and higher polyols on nickel display a remarkably selective production of formate. This efficient oxidative C–C bond cleavage on nickel is displayed in somewhat different fashion for partially oxidized C_2 reactants in that carbonate is predominantly formed. Some possible surface chemical factors responsible for these striking mechanistic differences are discussed.

Introduction

While often overlooked by chemists, electrochemistry can provide a highly controllable as well as flexible means with which to undertake redox-induced transformations of organic molecules. A limitation of purely electrochemical measurements, however, is that little specific information can be discerned regarding the identity of reaction intermediates and hence detailed reaction pathways. This difficulty can be circumvented in part by combining electrochemical methods with other techniques, such as optical and mass spectroscopies and chromatography. These additional techniques are often limited to postelectrolytic analysis, however, thereby being restricted largely to the identification of final reaction products.

The use of thin-layer electrochemistry combined with Fourier-transform infrared spectroscopy provides a relatively straightforward, yet powerful, means of providing real-time (ca. 1-s time scale) vibrational characterization of the solution as well as the surface electrode composition as such electrochemical processes proceed.[1-5] Given the well-known suitability of infrared spectroscopy for functional-group characterization, this tactic should constitute a quantitative means of assessing the kinetics of specific molecular transformations, thus providing a valuable adjunct to the overall reaction kinetics obtained from simultaneously acquired electrochemical data.[3a,d]

A simple variant of such real-time spectroelectrochemical measurements, utilized here, involves obtaining sequences of FTIR spectra during a single potential sweep or step. Subtraction of appropriate spectra is undertaken so to remove solvent and other interferences, exposing the potential-dependent components associated chiefly with the desired redox-induced changes in thin-layer solute composition. We have dubbed this type of procedure "single potential alteration infrared spectroscopy" (SPAIRS) to distinguish it from other potential-difference procedures that feature repeated modulations.[2] Within limits, such vibrational spectral information should become increasingly valuable as the complexity of the reaction pathway becomes greater. A number of such studies for both organic and inorganic redox systems have appeared recently;[1-5] however, the virtues of the approach from an organic mechanistic standpoint have yet to be fully exploited.

Outlined herein is a straightforward, yet we believe insightful, examination of electrooxidation pathways discerned in this fashion for ethylene glycol and related polyhydric alcohols in alkaline aqueous solution at polycrystalline gold, platinum, and nickel surfaces. Ethylene glycol is of interest not only as a possible candidate for fuel-cell development but also in view of extensive previous electrochemical examinations of its oxidation on platinum[2] and gold.[3] In spite of these activities, the oxidation mechanisms are poorly understood, in part with regard to the role of the several possible partly oxidized (aldehyde, carboxylate) species in the

† Present address: Dow Chemical Co., Midland, MI 48667.

(1) For a recent review, see: Christensen, P. A.; Hamnett, A. In *Comprehensive Chemical Kinetics*, Compton, R. G., Hamnett, A., Eds.; Elsevier: Amsterdam, 1989; Vol. 29, Chapter 2.

(2) Corrigan, D. S.; Leung, L.-W. H.; Weaver, M. J. *Anal. Chem.* **1987**, *59*, 2252.

(3) Recent examples from our laboratory for electroorganic processes: (a) Leung, L.-W. H.; Weaver, M. J. *J. Phys. Chem.* **1988**, *92*, 4019. (b) Leung, L.-W. H.; Chang, S.-C.; Weaver, M. J. *J. Electroanal. Chem.* **1989**, *266*, 317. (c) Leung, L.-W. H.; Weaver, M. J. *J. Phys. Chem.* **1989**, *93*, 7218. (d) Leung, L.-W. H.; Weaver, M. J. *Langmuir* **1990**, *6*, 323. (e) Chang, S.-C.; Leung, L.-W.; Weaver, M. J. *J. Phys. Chem.* **1990**, *94*, 6013.

(4) (a) Nishimura, K.; Kunimatsu, K.; Machida, K. I.; Enyo, M. *J. Electroanal. Chem.* **1989**, *260*, 181. (b) Sun, S. G.; Yang, D.-F.; Tian, Z.-W. *J. Electroanal. Chem.* **1990**, *289*, 177.

(5) For example, see: (a) Bullock, J. P.; Palazotto, M. C.; Mann, K. R. *Inorg. Chem.* **1991**, *30*, 1284. (b) Lewis, G. J.; Roth, J. D.; Safford, L. K.; Gao, X.; Chang, S.-C.; Dahl, L. F.; Weaver, M. J. *J. Am. Chem. Soc.* **1990**, *112*, 2831.

0002-7863/91/1513-9506$02.50/0